
JOURNAL OF THE AMERICAN CHEMICAL SOCIETY

Preparation of Carbosilane Dendrimers and Their Characterization Using $^1\text{H}/^{13}\text{C}/^{29}\text{Si}$ Triple Resonance 3D NMR Methods

Minghui Chai, Zhengjie Pi, Claire Tessier,* and Peter L. Rinaldi*

Contribution from the Department of Chemistry, 190 E. Buchtel Commons, Knight Chemical Laboratory,
The University of Akron, Akron, Ohio 44325-3601

Received September 4, 1998. Revised Manuscript Received November 12, 1998

Abstract: In this paper we show the utility of $^1\text{H}/^{13}\text{C}/^{29}\text{Si}$ triple resonance, 3D, and pulse field gradient (PFG) NMR techniques for characterizing organosilicon based polymers. The dendrimers studied are first generation $\text{Si}(\text{CH}_2\text{CH}_2\text{SiHMe}_2)_4$ and second generation $\text{Si}[\text{CH}_2\text{CH}_2\text{SiMe}(\text{CH}_2\text{CH}_2\text{SiHMe}_2)_2]_4$ polycarbosilanes. The signals from one-bond and two-bond connectivities among ^1H atoms coupled to both ^{13}C and ^{29}Si at natural abundance have been selectively detected. The spectral dispersion and the atomic connectivity information present in the 3D NMR spectra provide resonance assignments and a definitive structure proof.

Introduction

Over the past few years, macromolecules known as dendrimers have attracted great interest.¹ Starburst dendrimers are highly ordered, hyper-branched, oligomeric and polymeric molecules formed by multiplicative growth from a central core containing an increasing number of functional groups. They have three major architectural components: an initiator core, an interior, and an exterior. These three components are interdependent and control the size, shape, and chemical environment of dendrimers. The well-defined structures of dendrimers can provide new and unique physical and chemical properties such as low intrinsic viscosity, high solubility and miscibility, and high reactivity. These molecules provide new models for basic and theoretical studies, and they are able to lead to new applications which have been explored or developed including nanoscale catalysts and reaction vessels, micelle mimics, magnetic resonance imaging agents, drug and gene delivering agents, chemical sensors, information-processing materials, high performance

polymers, molecular weight or size standard precursors to star-branched polymers, as well as novel building blocks for nanotechnology. As a result, there is a growing need for improved spectroscopic methods to characterize their structures.

A number of polycarbosilane dendrimers have been reported, and several reviews have been published on this topic.² A repetitive alkenylation and hydrosilation cycle has been developed for the high-yield divergent synthesis of two- and three-carbon bridged carbosilane dendrimers up to the fifth generation.³⁻⁵ To generate a dendrimer with maximum symmetry, only the β -isomer of hydrosilation is desired. The presence of the α -isomer and missing arms due to incomplete hydrosilation or alkenylation are the expected imperfections in a carbosilane dendrimer.

(2) (a) Mathias, L. J.; Carothers, T. W. In *Advances in Dendritic Macromolecules*; Newkome, G. R., Ed.; JAI: Greenwich, Connecticut, 1995; Vol. 2, Chapter 4. (b) Cuadrado, I.; Morán, M.; Losada, J.; Casado, C. M.; Pasual, C.; Alonso, B.; Lobete, F. In *Advances in Dendritic Macromolecules*; Newkome, G. R., Ed.; JAI: Greenwich, Connecticut, 1995; Vol. 3, Ch. 4. (c) Gudat, D. *Angew. Chem., Int. Ed. Engl.* **1997**, *36*, 1951.

(3) van der Made, A. W.; van Leeuwen, P. W. N. M. *J. Chem. Soc., Chem. Commun.* **1992**, 1400.

(4) (a) Zhou, L.-L.; Roovers, J. *Macromolecules* **1993**, *26*, 963. (b) Zhou, L.-L.; Toporowski, P. M.; Roovers, J.; Hadjichristidis, N. *Rubber Chem. Technol.* **1992**, *65*, 303. (c) Roovers, J.; Toporowski, P. M.; Zhou, L.-L. *Polym. Prepr. (Am. Chem. Soc., Div. Polym. Chem.)* **1992**, *33(1)*, 182.

(1) (a) van der Made, A. W.; van Leeuwen, P. W. N. M.; de Wilde, J. C.; Brands, R. A. C. *Adv. Mater.* **1993**, *5*, 466. (b) Dagani, R. *Chem. Eng. News* **1996**, *74*, 20. (c) Service, R. F. *Science* **1995**, *267*, 458-459. (d) Newkome, G. R.; Morefield, C. N.; Vögtle, F. *Dendritic Molecules*; VCH: New York, 1996.

NMR has been a powerful tool for the structural analysis of macromolecules. 1D ^1H and ^{13}C NMR have been used in combination with other techniques such as elemental analysis and MS for characterizing the structures of dendrimers.⁶ 1D NMR of other nuclei has also been utilized for studying structures of dendrimers which contain atoms such as ^{15}N , ^{11}B , ^{29}Si , and ^{31}P nuclei.⁷ The conformation⁸ and shape⁹ of dendrimers, site-specifically labeled with NMR-active stable isotopes, have been studied by rotational-echo double resonance (REDOR) solid-state NMR techniques.^{8,9} To date, mainly 1D NMR techniques have been applied to dendrimer structure studies. The 1D NMR spectra of carbosilane dendrimers, which were first reported in 1992,³ are usually complicated because of the similar chemical environments of the three components of dendrimer structure. The characterization often requires combinations of several techniques. Multidimensional NMR techniques, especially inversely detected 3D heteronuclear shift correlation experiments, offer the opportunity to obtain the complete structural characterization by using NMR experiments alone. These experiments provide much more information than 1D experiments because they disperse resonances into three dimensions, enabling the resolution of signals from many additional species; they provide greatly enhanced sensitivity, enabling the detection of species which are present at very low concentrations; and they provide correlations which indicate atomic connectivities.

$^1\text{H}/^{13}\text{C}/^{15}\text{N}$ triple resonance 3D NMR techniques have been enormously useful for characterization of biopolymers such as proteins,¹⁰ however, the biological experiments are usually performed in conjunction with uniform ^{13}C and ^{15}N isotopic labeling. In polymer chemistry, when isotopic labeling is possible, it is often very difficult and expensive. By modifying the 3D pulse sequence used for biopolymers, triple resonance 3D NMR techniques have been adapted for studying the structures of polymers, which involve $^1\text{H}-^{13}\text{C}-^{19}\text{F}$,¹¹ $^1\text{H}-^{13}\text{C}-^{31}\text{P}$,¹² and $^1\text{H}-^{13}\text{C}-^{29}\text{Si}$ ¹³ spin systems. These results have shown that 3D NMR spectroscopy can be tremendously useful for characterizing polymer structures, even without isotopic labeling. In a recent communication,¹³ a 3D $^1\text{H}/^{13}\text{C}/^{29}\text{Si}$ triple resonance NMR method combined with pulse field gradients (PFG) were used to unambiguously determine the resonance assignments for mm, mr/rm, rr triad stereosequences in poly-(1-phenyl-1-silabutane)(PPSB). The $^1\text{H}/^{13}\text{C}/^{29}\text{Si}$ triple resonance NMR technique requires selective detection of the $^1\text{H}-^{13}\text{C}-^{29}\text{Si}$ spin systems, which are present in only 0.05% of the molecules, while suppressing the signals from the remaining

(5) (a) Seyferth, D.; Son, D. Y. *Organometallics* **1994**, *13*, 2682. (b) Seyferth, D.; Kugita, T. *Organometallics* **1995**, *14*, 5362.

(6) (a) Ihre, H.; Hult A.; Soederlind, E. *J. Am. Chem. Soc.* **1996**, *118*, 6388. (b) Kim, C.; Park, E.; Kang, E. *Bull. Korean Chem. Soc.* **1996**, *17*(7), 592–595. (c) Kim, R. M.; Bernick, A. M.; Champman, K. T. *Proc. Natl. Acad. Sci. U.S.A.* **1996**, *93*(19), 10012.

(7) (a) van Genderen, M. H. P.; Baars, M. W. P. L.; Elissen-Roman, C.; de Brabander van der Berg, E. M. M.; Meijer, E. W. *Polym. Mater. Sci. Eng.* **1995**, *73*, 336. (b) Smith, B. M.; Todd, P.; Bowman, C. N. *Polym. Mater. Sci. Eng.* **1996**, *75*, 331. (c) Ponomarenko, S. A.; Rebrov, E. A.; Bobrovsky, A. Y.; Boiko, N. I.; Muzafarov, A. M.; Shibaev, V. P. *Liq. Cryst.* **1996**, *21*(1), 1. (d) Catalano, V. J.; Parodi, N. *Inorg. Chem.* **1997**, *36*, 537.

(8) Wooley, K.; Klug, C.; Kowalewski, T.; Schaefer, J. *Polym. Mater. Sci. Eng.* **1995**, *73*, 230.

(9) Wooley, K.; Klug, C.; Iasaki, K.; Schaefer, J. *J. Am. Chem. Soc.* **1997**, *119*(1), 53.

(10) Cavanaugh, J.; Fairbrother, W.; Palmer, A. G., III; Skelton, N. *Protein NMR Spectroscopy*; Academic Press: London, 1995.

(11) Li, L.; Rinaldi, P. L. *Macromolecules* **1996**, *29*, 4808.

(12) Saito, T.; Medesker, R. E.; Harwood, H. J.; Rinaldi, P. L. *J. Magn. Reson., Ser. A* **1996**, *120*, 125.

(13) Chai, M.; Saito, T.; Pi, Z.; Tessier, C.; Rinaldi, P. L. *Macromolecules* **1997**, *30*, 1240.

99.95% of molecules. It is an extremely challenging experiment; however, modern instrumentation and a stable instrument environment make the experiment feasible. In this paper, a description of the technique is provided, and we apply it to the characterization of carbosilane dendrimers **1** ($\text{Si}[\text{CH}_2\text{CH}_2\text{SiHMe}_2]_4$), and **2** ($\text{Si}[\text{CH}_2\text{CH}_2\text{SiMe}(\text{CH}_2\text{CH}_2\text{SiHMe}_2)_2]_4$). The information obtained from the 3D NMR allows the complete assignments of the resonances from both dendrimers.

Experimental Section

General Comments. Unless otherwise specified, all of the reactions and manipulations were carried out using standard anaerobic techniques.¹⁴ All of the solvents were purified and dried by standard procedures prior to use. *Addition of reaction mixtures that contain LiAlH_4 to aqueous acid must be done slowly and with caution.*

Materials. The Karstedt catalyst (platinum(0)-1,3-divinyl-1,1,3,3-tetramethyldisiloxane)¹⁵ was obtained from Gelest as a 2.1–2.4% solution in xylene. Dimethylchlorosilane, methyldichlorosilane, trivinylmethylsilane, and tetravinylsilane were purchased from Gelest and distilled from anhydrous Na_2CO_3 (for chlorosilanes) or 4 Å molecular sieves before use. Lithium aluminum hydride and vinylmagnesium bromide (Aldrich) were used as received without further purification. The compounds $\text{Si}(\text{CH}_2\text{CH}_2\text{SiMe}_2\text{Cl})_4$ and $\text{Si}(\text{CH}_2\text{CH}_2\text{SiMe}(\text{CH}=\text{CH}_2)_2)_4$ were prepared according to literature procedures.^{4,5}

Preparation of $\text{Si}(\text{CH}_2\text{CH}_2\text{SiMe}_2\text{H})_4$ (1**).** A solution of $\text{Si}(\text{CH}_2\text{CH}_2\text{SiMe}_2\text{Cl})_4$ (5.14 g, 10 mmol) in 20 mL of toluene was added slowly into an ice-cooled suspension of LiAlH_4 (0.76 g, 20 mmol, 100% excess) in 50 mL of diethyl ether. The mixture was stirred overnight at room temperature and refluxed for 1 h. The rest of the procedure was conducted in air. The mixture was filtered through Celite, and the filtrate was added *cautiously* to 80 mL of ice-cooled 2 N HCl. The aqueous layer was extracted twice with diethyl ether, and the organic layer was washed twice with water and once with saturated aqueous NaCl. The organic layer was dried over anhydrous MgSO_4 for a few hours and filtered through a pad of silica gel. Removal of volatiles at reduced pressure left 2.63 g (70%) of **1** as a clear colorless liquid. IR (neat) $\nu(\text{Si}-\text{H})$ 2112 cm^{-1} ; ^1H NMR (C_6D_6) δ 4.15 (m, 4 H), 0.60 (m, 16 H), 0.08 (d, 24 H); ^{13}C NMR (C_6D_6) δ 7.2, 4.4, -4.3; ^{29}Si NMR (C_6D_6) δ 9.8 (Si_I), -9.5 (Si_{II}).

Preparation of $\text{Si}[\text{CH}_2\text{CH}_2\text{SiMe}(\text{CH}_2\text{CH}_2\text{SiMe}_2\text{Cl})_2]_4$. A 50 mL flask equipped with a reflux condenser and a magnetic stirring bar was charged with 3.0 g (5.68 mmol) of $\text{Si}(\text{CH}_2\text{CH}_2\text{SiMe}(\text{CH}=\text{CH}_2)_2)_4$, 20 mL of diethyl ether, and 6 drops of Karstedt's catalyst solution. Me_2SiHCl (7.55 g, 79.5 mmol, 75% excess) was transferred into the flask at -78 °C. The mixture was warmed to room temperature, stirred for an additional 0.5 h at room temperature, and then heated for 20 h at 50 °C. Volatiles were removed at reduced pressure to leave 7.31 g (100%) of $\text{Si}[\text{CH}_2\text{CH}_2\text{SiMe}(\text{CH}_2\text{CH}_2\text{SiMe}_2\text{Cl})_2]_4$ as a white oily solid. ^1H NMR (C_6D_6) δ 0.73 (m, 48 H), 0.32 (s, 48 H), 0.08 (s, 12 H); ^{13}C NMR (C_6D_6) δ 12.2, 5.6, 4.6, 3.5, 1.3, -6.0; ^{29}Si NMR (C_6D_6) δ 32.7 (Si_{III}), 10.2 (Si_I), 8.9 (Si_{II}); MS(ED): m/z 289 (M - $\text{C}_4\text{H}_{11}\text{Si}$), 290 (M - $\text{C}_4\text{H}_{10}\text{Si}$).

Preparation of $\text{Si}[\text{CH}_2\text{CH}_2\text{SiMe}(\text{CH}_2\text{CH}_2\text{SiMe}_2\text{H})_2]_4$ (2**).** A solution of $\text{Si}[\text{CH}_2\text{CH}_2\text{SiMe}(\text{CH}_2\text{CH}_2\text{SiMe}_2\text{Cl})_2]_4$ (6.42 g, 5 mmol) in 20 mL of diethyl ether was added slowly into an ice-cooled suspension of LiAlH_4 (0.76 g, 20 mmol, 100% excess) in 50 mL of diethyl ether. The mixture was stirred overnight at room temperature and refluxed for 1 h. The workup of the reaction was conducted in air. The mixture was filtered through Celite, and the volatiles were removed at reduced pressure. Pentane (50 mL) was added, followed by filtration, removal of volatiles, and another cycle of extraction. The residual aluminum compounds were washed away with 5–10 mL of CH_3CN . *Caution: exothermic!* Removal of volatiles at reduced pressure left 3.78 g (75%) of **2** as a colorless viscous liquid. Compound **2** was stored under nitrogen or argon. IR (neat) $\nu(\text{Si}-\text{H})$ 2112 cm^{-1} ; ^1H NMR (C_6D_6) δ

(14) (a) Shriver, D. F.; Drezdson, M. A. *The Manipulation of Air-Sensitive Compounds*, 2nd ed.; Wiley: New York, 1986. (b) Errington, R. J. *Advanced Practical Inorganic and Metalorganic Chemistry*; Blackie Academic & Professional: New York, 1997.

(15) Karstedt, B. Q. U.S. Patent 3,775,452, 1973.

4.18 (m, 8 H), 0.74 (m, 16 H), 0.63 (m, 32 H), 0.11 (d, 48 H), 0.10 (s, 12 H); ^{13}C NMR (C_6D_6) δ 7.3, 6.2, 5.9, 3.6, -4.3, -5.8; ^{29}Si NMR (C_6D_6) δ 10.2 (Si_I), 8.2 (Si_{II}), -9.8 (Si_{III}); MS (MALDI) $[\text{M} + \text{Ag}]^+ m/z$ 1115.5 (54, calcd. 1115.5) 1116.5 (61), 1117.5 (100), 1118.5 (90), 1119.4 (83) 1120.5 (42), 1121.5 (25).

NMR Measurements. The routine 1D ^{13}C and ^{29}Si NMR spectra were collected at ambient temperature on a Varian VXR300 300 MHz spectrometer. The 1D, 2D, and 3D ^1H NMR spectra were collected at 30 °C on a Varian Unityplus 600 MHz NMR spectrometer equipped with a Nalorac 5 mm $^1\text{H}/^2\text{H}/^{13}\text{C}/\text{X}$ (where X is tuneable over the range of the resonance frequencies from ^{15}N to ^{31}P) pulse field gradient probe. C_6D_6 was used as the solvent as well as the internal reference for ^1H and ^{13}C chemical shifts. TMS was used as an external reference for ^{29}Si chemical shifts.

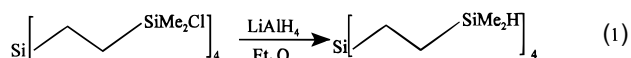
1D NMR. The ^1H spectra of both dendrimers were acquired at 600 MHz using a 1.9 s acquisition time, 3.3 μs (30°) pulse width and 16 transients. The ^{13}C spectra of both dendrimers were acquired at 75 MHz with Waltz-16 modulated ^1H decoupling using a 1.8 s acquisition time, 6.4 μs (45°) pulse width and 256 transients. The ^{29}Si spectra of both dendrimers were acquired at 60 MHz with Waltz-16 modulated ^1H decoupling using a 3.0 s acquisition time, 3.0 μs (30°) pulse width, 15 s delay and 128 transients.

3D NMR. 3D NMR spectra of **1** were collected with ^1H , ^{13}C , and ^{29}Si 90° pulses of 10.8, 21.0, and 12.0 μs , respectively; a relaxation delay of 1.5 s, $\Delta = 1.78$ ms ($1/(4 \times ^1J_{\text{CH}})$), $\tau = 35.7$ ms ($1/(4 \times ^2J_{\text{CSi}})$), $^2J_{\text{CSi}} = 7$ Hz) for two-bond C–Si correlation and $\tau = 4.24$ ms ($1/(4 \times ^1J_{\text{CSi}})$), $^1J_{\text{CSi}} = 59$ Hz) for one-bond C–Si correlation, an acquisition time = 0.058 s (with simultaneous ^{13}C MPF-7 and ^{29}Si MPF-7 decoupling). Four transients were averaged for each of 2×16 increments during t_1 and 2×14 increments during t_2 according to the method of States et al.,¹⁶ a 1668.6 Hz spectral window in f_3 , a 2706.4 Hz spectral window in f_1 , and a 1432.2 Hz spectral window in f_2 . The durations and amplitudes of the gradient pulses were 3, 1, and 1 ms and 0.303, 0.243, and 0.048 T/m, respectively. The first gradient pulse serves as a homospoil pulse; therefore, its value relative to the others is not critical. The ratio of the areas of the second and the third gradient pulses is determined by the ratio of the ^1H and ^{29}Si resonance frequencies. The total experiment time was 5.5 h for the one-bond CSi correlation experiment and 5.75 h for two-bond CSi correlation experiment. The data were zero filled to $256 \times 256 \times 256$ and weighted with a shifted sine bell function before Fourier transformation.

3D NMR spectra of **2** were collected with ^1H , ^{13}C , and ^{29}Si 90° pulses of 10.7, 21.0, and 13.0 μs , respectively. Other parameters were identical to those described above for **1**. To enhance the resolution of the 3D NMR spectra without increasing the data set size, the ^{29}Si spectral window was narrowed so that the strong ^{29}Si signals from Si-(II) in **1** and Si(III) in **2** folded into a region of the narrow spectral window used for the 3D experiments where they do not overlap with other resonances. The chemical shifts of the folded peaks are corrected, depending on the values from 1D ^{29}Si spectra for both dendrimers.

Results and Discussion

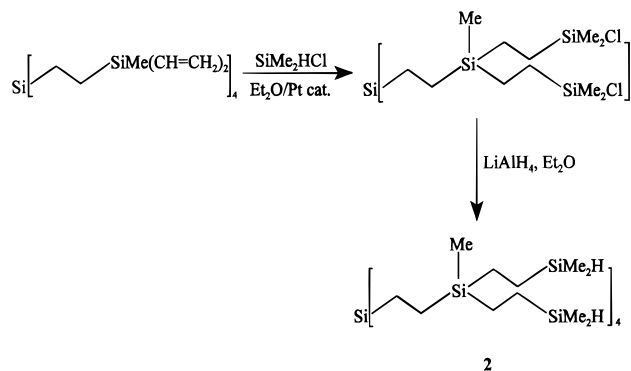
Preparation of Dendrimers. The divergent synthetic routes for the preparation of two-carbon spacer carbosilane dendrimers include three types of reactions: hydrosilylation, vinylation with excess vinylmagnesium bromide, and reduction of Si–Cl with LiAlH_4 . This series of steps has been used by Roovers⁴ and Seyferth⁵ in the synthesis of other two-carbon spacer carbosilane dendrimers. The first generation dendrimer $\text{Si}(\text{CH}_2\text{CH}_2\text{SiMe}_2\text{H})_4$ (**1**) was prepared by LiAlH_4 reduction of the known chloride $\text{Si}(\text{CH}_2\text{CH}_2\text{SiMe}_2\text{Cl})_4$ (eq 1).



The second-generation dendrimer $\text{Si}(\text{CH}_2\text{CH}_2\text{SiMe}(\text{CH}_2\text{CH}_2\text{SiMe}_2\text{H})_2)_4$ (**2**) was prepared from the known octavinyl com-

(16) States, D. J.; Haberkorn, R. A.; Ruben, D. J. *J. Magn. Reson.* **1982**, *48*, 286.

Scheme 1



pound $\text{Si}(\text{CH}_2\text{CH}_2\text{SiMe}(\text{CH}=\text{CH}_2)_2)_4$ through the intermediacy of the octachloride $\text{Si}(\text{CH}_2\text{CH}_2\text{SiMe}(\text{CH}_2\text{CH}_2\text{SiMe}_2\text{Cl})_2)_4$ (Scheme 1). The hydrosilylation was conducted using Karstedt's catalyst¹⁵ in diethyl ether. The attempted conversion of $\text{Si}(\text{CH}_2\text{CH}_2\text{SiMe}(\text{CH}_2\text{CH}_2\text{SiMe}_2\text{Cl})_2)_4$ to **2**, employing an aqueous workup, gave extensively cross-linked product. Presumably, the aqueous workup resulted in the formation of Si–OH groups that reacted to give Si–O–Si linkages.¹⁷ An alternative nonaqueous workup was developed for **2** which takes advantage of its unique solubility properties. Extraction of the reaction mixture with hexane gave a mixture of **2** and aluminum salts. Acetonitrile was carefully added (exothermic) to extract the aluminum salts from the virtually insoluble **2**. Compound **2** can be handled in air for short periods but, because of its mild air-sensitivity, it should be stored under argon or nitrogen.

Compounds **1** and **2** were characterized by mass spectrometry. EI mass spectrometry of **1** showed two major fragments at mass 289 and 290 in which it appears loss of one arm of **1** has taken place. The fragments can be assigned to $\text{Si}(\text{CH}_2\text{CH}_2\text{SiMe}_2\text{H})_3^+$ and $\text{HSi}(\text{CH}_2\text{CH}_2\text{SiMe}_2\text{H})_3$. MALDI mass spectrometry has been reported to be a useful technique for the characterization of carbosilane dendrimers.¹⁸ Although compound **1** was too volatile for MALDI mass spectrometry, this technique was useful for **2**. The monoisotopic peak for $\text{Ag}(\mathbf{2})^+$ was found at m/z 1115.5 (calcd m/z 1115.5). The isotopic distribution of peaks for $\text{Ag}(\mathbf{2})^+$ was as expected.

NMR Characterization of Dendrimer 1. From the core to the exterior of the dendrimer, silicon atoms are marked as Si-(I), Si(II), and Si(III); the methylene groups are labeled as $\alpha_{\text{I}}\text{-CH}_2$, $\beta_{\text{I}}\text{-CH}_2$ and $\alpha_{\text{II}}\text{-CH}_2$, $\beta_{\text{II}}\text{-CH}_2$; the methyl group are identified as $\text{CH}_3(\text{II})$ and $\text{CH}_3(\text{III})$ based on the identity of the closest Si atom.

1D Spectra. Parts a–c of Figure 1 show the 1D ^1H , ^{13}C , and ^{29}Si NMR spectra of **1**. The ^1H NMR spectrum contains three major groups of resonances: the silicon hydride proton peak at 4.12 ppm, the methyl resonances at ca. 0.06 ppm, and the methylene protons at 0.53–0.59 ppm. The ^{13}C spectrum shows three resonances which arise from the methyl (–4.34 ppm) and methylene (4.44 and 7.27 ppm) carbons. The ^{29}Si spectrum displays two well-resolved resonances which can be assigned as Si(I) (core-silicon) at 9.39 ppm and Si(II) (outer-silicon) at –9.80 ppm on the basis of their relative intensities. Because the ^{29}Si chemical shifts are well-resolved, it is possible to obtain ^1H and ^{13}C resonance assignments by using multidimensional

(17) (a) Mathias, L. J.; Carothers, T. W. *J. Am. Chem. Soc.* **1991**, *113*, 4043. (b) Boury, B.; Corriu, R. J. P.; Leclercq, D.; Mutin, P. H.; Planeix, J.-M.; Vioux, A. *Organometallics* **1991**, *10*, 1457.

(18) Three examples: (a) Wu, Z.; Biemann, K. *Int. J. Mass Spectrom. Ion Processes* **1997**, *165/166*, 349. (b) Frey, H.; Lorenz, K.; Müllhaupt, R. U.; Mayer-Posner, F. *J. Macromol. Symp.* **1996**, *102*, 19. (c) Krksa, S. W.; Seyferth, D. *J. Am. Chem. Soc.* **1998**, *120*, 3604.

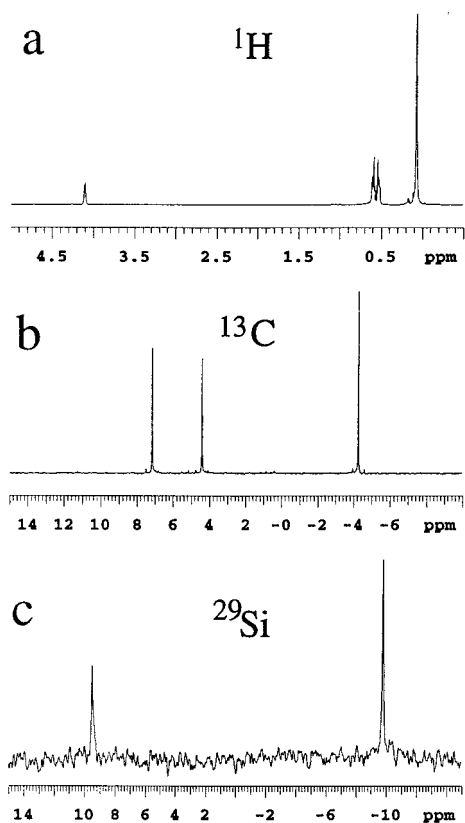


Figure 1. 1D NMR spectra of first generation dendrimer **1**: (a) 600 MHz ^1H spectrum; (b) 75 MHz ^{13}C spectrum; (c) 59.9 MHz ^{29}Si spectrum.

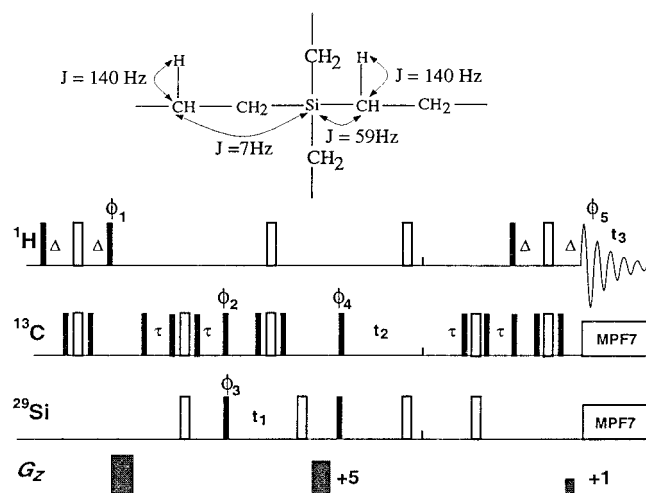


Figure 2. Diagram of the pulse sequence used to obtain the $^1\text{H}/^{13}\text{C}/^{29}\text{Si}$ triple resonance 3D NMR correlation spectra: $\Phi_1 = y$, $\Phi_2 = (x)_4, (y)_4, (-x)_4, (-y)_4$; $\Phi_3 = x, -x$; $\Phi_4 = y, y, -y, -y$; $\Phi_5 = x, -x, -x, x$; Φ_3 is incremented during t_1 , and Φ_4 is incremented during t_2 to provide a hypercomplex phase sensitive 3D data set.¹⁶

mensional NMR experiments which disperse signals based on the ^{29}Si chemical shifts. With the exception of the α - and β -methylene resonances, the 1D spectra of **1** can be assigned by inspection. However, this structure serves as a good illustration of the use of 3D NMR techniques for structural assignment, and the interpretation of the spectrum provides a definitive structure proof.

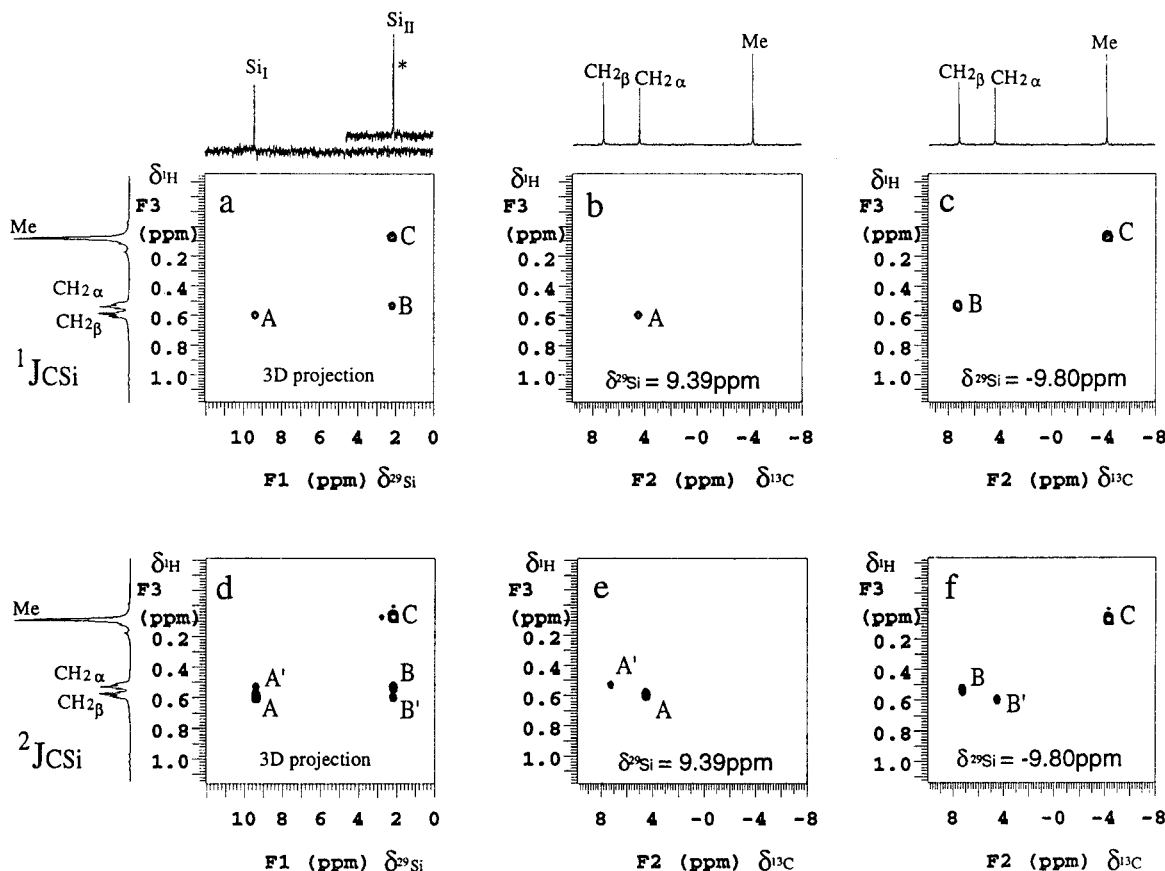
3D-NMR Pulse Sequence. Figure 2 shows the pulse sequence used for the $^1\text{H}/^{13}\text{C}/^{29}\text{Si}$ 3D correlation experiment. The theory explaining the operation of this sequence has been described using the $^1\text{H}/^{13}\text{C}/^{31}\text{P}$ spin system.¹² The important

features of this experiment are that pulses are applied to the ^1H , ^{13}C , and ^{29}Si frequencies, permitting selective detection of the 0.05% of the molecules containing these three isotopes in a specific bonding relationship. The experiment involves excitation and detection of ^1H NMR magnetization producing a factor of $(\gamma_{\text{H}}/\gamma_{\text{Si}})^{5/2} = 56$ (where γ_{H} and γ_{Si} are the gyromagnetic ratios of ^1H and ^{29}Si , respectively) increase in signal strength compared to experiments which involve excitation and detection of ^{29}Si NMR magnetization. Magnetic field gradients are applied along the z -axis to selectively refocus magnetization from $^1\text{H}/^{13}\text{C}/^{29}\text{Si}$ three-spin systems, while destroying all other magnetization. Because it is ^1H magnetization which is excited and detected, the shorter relaxation times of the ^1H 's determine the repetition time of the experiment rather than the longer relaxation times of the atoms ^{29}Si .

Normally, the Δ delay is set on the basis of the one-bond C–H coupling. From there, the experiment can be performed in a number of ways to obtain different structural information. If the τ delays are set on the basis of one-bond C–Si couplings (ca. 60 Hz), then the 3D NMR spectrum will produce correlations among the Si, α -C, and α -H atoms, identifying Si–C–H fragments. However, if the τ delays are set on the basis of two-bond C–Si couplings (ca. 5–10 Hz), then the 3D NMR spectrum will produce correlations among the Si, β -C, and β -H atoms, identifying Si–C–C–H fragments. Combined data from the two experiments provides more than enough information to identify the bonding network throughout the molecule. If defects exist due to the fact that all of the arms do not grow to the same length, then the atomic connectivities obtained from the 3D NMR spectra will reach a dead end before the chain is completed.

3D NMR Spectra of 1. Figure 3 shows plots from the 3D NMR spectra of **1**. Parts a–c of Figure 3 are from the spectrum obtained with τ delays optimized for one-bond C–Si couplings. Figure 3a contains the projection of the entire spectrum onto the f_1/f_3 plane and exhibits correlations between Si and α protons. Si_I has only α -methylene protons (cross-peak A); however, Si_{II} has both α -methylene (cross-peak B) and α -methyl (cross-peak C) protons. Note that to minimize the size of the 3D NMR data set, the spectral window in the f_1 dimension was narrowed so that the resonances from Si_{II} fold into the spectrum from -9.80 ppm. Figure 3b and c contains f_2/f_3 planes from the 3D NMR spectrum at f_1 positions corresponding to the ^{29}Si shifts of Si_I (9.39 ppm) and Si_{II} (-9.80 ppm), showing C–H correlations from the CH_n groups bound to Si_I and Si_{II}, respectively. Cross-peak A in Figure 3b is attributed to α -CH₂; cross-peaks B and C in Figure 3c are attributed to β -CH₂, and CH₃ groups, respectively.

Parts d–f of Figures 3 are from the 3D NMR spectrum of **1** obtained with τ delays optimized for two-bond C–Si couplings (assuming 7 Hz). Figure 3d contains the projection of the entire spectrum onto the f_1/f_3 plane and exhibits correlations between H and Si. Three cross-peaks, A, B, and C, are present from correlations between Si and H in Si–C–H structure fragments. Additionally, cross-peaks A', B', and C' are present, resulting from correlations between Si and H in Si–C–C–H structure fragments. This latter group of peaks are expected since the 3D NMR experiment was performed with delays optimized for two-bond C–Si couplings. The former group of peaks are residual correlations from one-bond C–Si couplings which are not entirely removed from the spectrum with the sequence used. Although there are methods to effectively eliminate these peaks, the 3D spectral dispersion is adequate so that their presence does not interfere with the interpretation of the data.



* The ^{29}Si resonance is folded from the $\delta = -9.80$ ppm (see experimental)

Figure 3. $^1\text{H}/^{13}\text{C}/^{29}\text{Si}$ 3D NMR spectra of first generation dendrimer **1**: (a) 3D f_1/f_3 projection of the one-bond C—Si $^1\text{H}/^{13}\text{C}/^{29}\text{Si}$ 3D NMR spectrum; (b–c) f_2/f_3 slices at different ^{29}Si chemical shifts from the one-bond C—Si $^1\text{H}/^{13}\text{C}/^{29}\text{Si}$ 3D NMR spectrum: (b) f_2/f_3 slice at $\delta^{29}\text{Si} = 9.39$ and (c) f_2/f_3 slice at $\delta^{29}\text{Si} = -9.80$; (d) 3D f_1/f_3 projection of the multiple-bond C—Si $^1\text{H}/^{13}\text{C}/^{29}\text{Si}$ 3D NMR spectrum; (e–f) f_2/f_3 slices at different ^{29}Si chemical shifts from the two-bond C—Si $^1\text{H}/^{13}\text{C}/^{29}\text{Si}$ 3D NMR spectrum; (e) f_2/f_3 slice at $\delta^{29}\text{Si} = 9.39$ and (f) f_2/f_3 slice at $\delta^{29}\text{Si} = -9.80$.

Table 1. Chemical Shifts Assignment for **1** and **2**

first generation dendrimer (1)			second generation of dendrimer (2)		
$\delta^{29}\text{Si}$	$\delta^1\text{H}$	$\delta^{13}\text{C}$	$\delta^{29}\text{Si}$	$\delta^1\text{H}$	$\delta^{13}\text{C}$
	$\alpha_1\text{-CH}_2$ 0.59			$\alpha_1\text{-CH}_2$ 0.73	$\alpha_1\text{-CH}_2$ 3.59
Si(I) 9.39	$\beta_1\text{-CH}_2$ 0.53	$\alpha_1\text{-CH}_2$ 4.44	Si(I) 9.95	$\beta_1\text{-CH}_2$ 0.70	$\beta_1\text{-CH}_2$ 6.28
		$\beta_1\text{-CH}_2$ 7.27		$\alpha_{II}\text{-CH}_2$ 0.64	$\alpha_{II}\text{-CH}_2$ 5.99
Si(II) -9.80	CH_3 (I) 0.06	CH_3 (I) -4.34	Si(II) 7.99	$\beta_{II}\text{-CH}_2$ 0.59	$\beta_{II}\text{-CH}_2$ 7.41
	H—Si 4.12		Si(III) -9.83	CH_3 (I) 0.06	CH_3 (I) -5.89
				CH_3 (II) 0.11	CH_3 (II) -4.33
				H—Si 4.12	

Figures 3e and 3f contain f_2/f_3 planes from the 3D NMR spectrum at f_1 positions corresponding to the ^{29}Si shifts of Si_I (9.39 ppm) and Si_{II} (-9.80 ppm), showing C—H correlations from the CH_n groups two bonds from Si_I and Si_{II} , respectively. Note that the A/A' pair of peaks and the B/B' pair of peaks are clearly resolved in the 3D NMR planes, even though these peaks in Figure 3d are not resolved in the equivalent of a 2D NMR spectrum. Cross-peak A' in Figure 3e is from the β -methylene which is two bonds from Si_I . This cross-peak corresponds to cross-peak B in Figure 3c, which also identifies it as the methylene directly bound to Si_{II} . Cross-peak B' in Figure 3f is from the α -methylene which is two bonds from Si_{II} . This cross-peak also corresponds to cross-peak A in Figure 3b, which also identifies it as the methylene directly bound to Si_I . These resonance assignments together with exact chemical shifts are summarized in Table 1.

NMR Characterization of Dendrimer **2**. 1D NMR Spectra.

Figure 4 shows the 1D ^1H , ^{13}C , and ^{29}Si NMR spectra of **2**. These spectra are all considerably more complex when compared with the spectra of **1**. The ^1H spectrum (Figure 4a) exhibits three major groups of resonances: the silicon hydride proton at 4.12 ppm, the methylene protons between 0.5 and 0.75 ppm, and two methyl protons between 0.06 and 0.20 ppm. In this spectrum it is not possible to resolve and assign the $\alpha_1\text{-CH}_2$, $\beta_1\text{-CH}_2$, $\alpha_{II}\text{-CH}_2$, and $\beta_{II}\text{-CH}_2$ from the 1D spectrum. From the relative intensities of the methyl resonances, it is possible to assign CH_3 (II) and CH_3 (III) proton resonances to the signals at 0.06 and 0.11 ppm, respectively. The ^{13}C spectrum contains six resonances from the six nonequivalent carbons in **2**. However, the 1D spectrum does not contain enough information for their assignment. The ^{29}Si spectrum contains three resonances which correspond to Si (I), Si (II), and Si (III) at 9.95 ppm, 7.99 ppm,

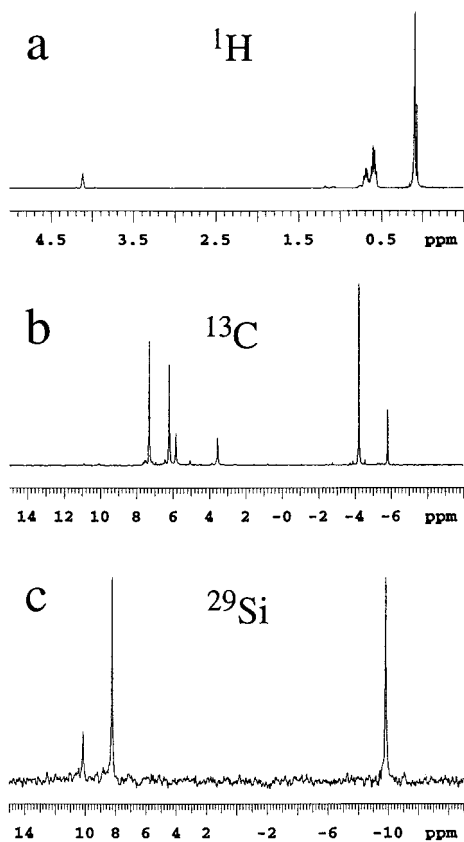


Figure 4. 1D NMR spectra of second generation dendrimer **2**: (a) 600 MHz ^1H spectrum; (b) 75 MHz ^{13}C spectrum; (c) 59.9 MHz ^{29}Si spectrum.

and -9.83 ppm, respectively. These assignments could be inferred from their relative intensities and comparison with the spectrum of **1** in Figure 1c.

3D NMR Spectra of 2. Figure 5 shows plots from the 3D NMR spectra of **2**, with the corresponding regions from the 1D ^1H , ^{13}C , and ^{29}Si spectra plotted along the horizontal and vertical axes. One set of plots (Figure 5a–d) is from the spectrum obtained with τ delays optimized for one-bond ^{13}C – ^{29}Si couplings, and the second set of plots (Figure 5e–h) is from the spectrum obtained with τ delays optimized for two-bond ^{13}C – ^{29}Si couplings. The f_1f_3 projections from both the one-bond (Figure 5a) and multiple-bond (Figure 5e) spectra give well-resolved peaks for all of the ^1H – ^{29}Si correlations. Parts b–d of Figure 5 show f_2f_3 slices ($^1\text{H}/^{13}\text{C}$ correlations) from the 3D $^1\text{H}/^{13}\text{C}/^{29}\text{Si}$ spectrum at the three ^{29}Si chemical shifts of **2**: Si_I at 9.95 ppm, Si_II at 7.99 ppm, and Si_III at -9.83 ppm. The f_2f_3 slice at $\delta^{29}\text{Si} = 9.95$ (Figure 5b), which is attributed to groups bound to Si_I , shows only one cross-peak (A) which arises from the ^1H – ^{13}C correlation of the four α - CH_2 's. In the slice at $\delta^{29}\text{Si} = 7.99$ (Figure 5c) corresponding to Si_II , there are three cross-peaks (B–D) from three different CH_n groups. Cross-peaks B and C are from two different methylene groups, and cross-peak D is from a methyl group as expected for Si_II . In the slice corresponding to $\delta^{29}\text{Si} = -9.83$ (Figure 5d), which is attributed to Si_III , there are two cross-peaks, E which is attributed to β - CH_2 and F which is attributed to Me_III .

The projection and slices from the two-bond experiment contain cross-peaks from the CH_n groups two bonds from Si and residual cross-peaks from CH_n groups directly bound to Si. The f_2f_3 slice at $\delta^{29}\text{Si} = 9.95$ (Figure 5f), which is attributed to groups bound to Si_I , shows a cross-peak A, which is attributed to the α - CH_2 as described above, and a cross-peak B from the β - CH_2 . This latter cross-peak corresponds to the position of cross-peak B in Figure 5c. These combined data prove the chain of atomic connectivities Si_I – α - CH_2 – β - CH_2 – Si_II .

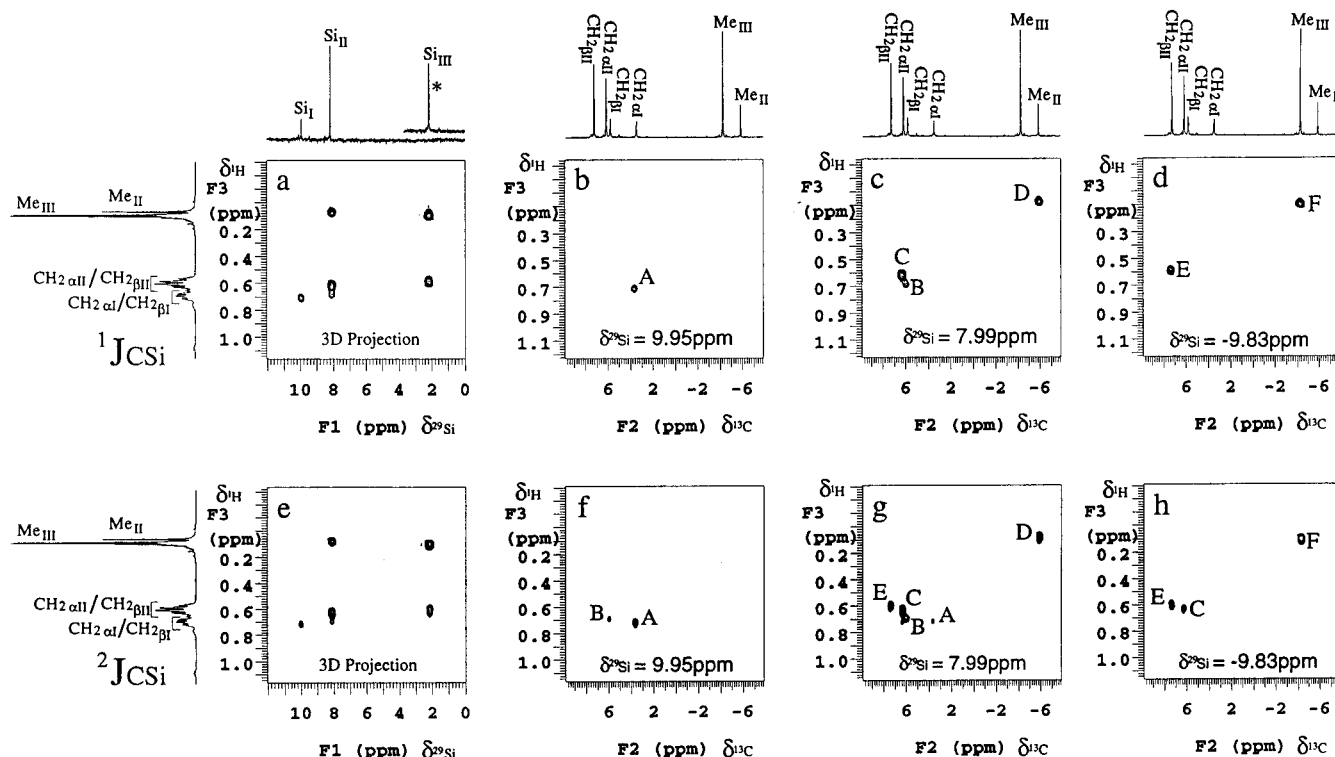


Figure 5. $^1\text{H}/^{13}\text{C}/^{29}\text{Si}$ 3D NMR spectra of second generation dendrimer **2**: (a) 3D f_1f_3 projection of the one-bond C–Si $^1\text{H}/^{13}\text{C}/^{29}\text{Si}$ 3D NMR spectrum; (b–d) f_2f_3 slices from the one-bond C–Si $^1\text{H}/^{13}\text{C}/^{29}\text{Si}$ 3D NMR spectrum: (b) f_2f_3 slice at $\delta^{29}\text{Si} = 9.95$, (c) f_2f_3 slice at $\delta^{29}\text{Si} = 7.99$, and (d) f_2f_3 slice at $\delta^{29}\text{Si} = -9.83$; (e) 3D f_1f_3 projection of the two-bond C–Si $^1\text{H}/^{13}\text{C}/^{29}\text{Si}$ 3D NMR spectrum; (f–h) f_2f_3 slices from the two-bond C–Si $^1\text{H}/^{13}\text{C}/^{29}\text{Si}$ 3D NMR spectrum: (f) f_2f_3 slice at $\delta^{29}\text{Si} = 9.39$, (g) f_2f_3 slice at $\delta^{29}\text{Si} = 7.99$, and (h) f_2f_3 slice at $\delta^{29}\text{Si} = -9.83$.

The f_2f_3 slice from the two-bond spectrum at $\delta^{29}\text{Si} = 7.99$ (Figure 5g), which is attributed to groups bound to Si_{II} , shows three cross-peaks B, C, and D which are attributed to $\beta_{\text{I}}\text{-CH}_2$, $\alpha_{\text{II}}\text{-CH}_2$, and Me_{II} groups, respectively, as determined from the one-bond experiment described above; and two new cross-peaks, A and E, from CH_n groups two bonds from Si_{II} . Cross-peak A is in the same position as cross-peak A from the Si_{I} slice in the one-bond experiment (Figure 5b). Therefore, these data establish the $\text{Si}_{\text{II}}\text{-}\beta_{\text{I}}\text{-CH}_2\text{-}\alpha_{\text{I}}\text{-CH}_2\text{-Si}_{\text{I}}$ connectivities. Cross-peak E is in the same position as cross-peak E from the Si_{III} slice in the one-bond experiment (Figure 5d). Therefore, these data establish the $\text{Si}_{\text{II}}\text{-}\alpha_{\text{II}}\text{-CH}_2\text{-}\beta_{\text{II}}\text{-CH}_2\text{-Si}_{\text{III}}$ connectivities.

Similarly, the f_2f_3 slice from the two-bond spectrum corresponding to $\delta^{29}\text{Si} = -9.83$ ppm (Figure 5h), which is attributed to groups bound to Si_{III} , shows two cross-peaks E and F which are attributed to $\beta_{\text{II}}\text{-CH}_2$ and Me_{III} groups, respectively, as determined from the one-bond experiment described above; and a new cross-peak, C, from CH_n groups two bonds from Si_{III} . Cross-peak C is in the same position as cross-peak C from the Si_{II} slice in the one-bond experiment (Figure 5c). Therefore, these redundant data confirm the $\text{Si}_{\text{II}}\text{-}\alpha_{\text{II}}\text{-CH}_2\text{-}\beta_{\text{II}}\text{-CH}_2\text{-Si}_{\text{III}}\text{-Me}_{\text{III}}$ connectivities.

Complete atomic connectivities and ^1H , ^{13}C , and ^{29}Si chemical shift assignments of **2** are thus obtained, which are summarized in Table 1.

If all of the arms of the dendrimer had not grown to the same degree, then additional structure fragments would have been identified from the 3D NMR correlations. On the basis of the the experiment time and signal-to-noise in these spectra, it is estimated that dendrimers up to fourth or fifth generation might be characterized with these NMR methods or that impurities at the level of 5–10% from incomplete growth of one of the dendrimer arms might be detected. If ^{13}C or ^{29}Si isotopic labeling

were employed, then much lower concentrations of species might be detected.

Conclusion

Triple-resonance PFG-3D NMR experiments can be tremendously useful for studying macromolecules without resorting to isotopic labeling, even when the nuclei involved are present in low natural abundance. On the basis of the the better sensitivity of ^{29}Si chemical shift to structural variations, ^1H and ^{13}C resonances can be resolved through the 3D $^1\text{H}/^{13}\text{C}/^{29}\text{Si}$ NMR correlation experiment. By dispersing resonances into three dimensions, it is possible to resolve similar methylene resonances, when signals overlap in 1D and 2D NMR spectra. Once these resonances are resolved, the unique ability of 3D NMR experiments to simultaneously relate the shifts of three coupled nuclei provides unequivocal assignments for all of the resonances of both generations of carbosilane dendrimers. These techniques can also be useful for characterizing star-branched polymers which contain an NMR-active nucleus, polymers with low concentrations of heteroatoms (e.g., at the chain-end or at low-occurrence branch point), and many organometallic compounds. Although the methods are used here to study Si-containing polymers, the technique could be extended to include any NMR-active nuclei which exhibit J -coupling to ^{13}C .

Acknowledgment. We thank Professor Chrys Wesdemiotis for the mass spectral data and Mr. Joseph Hrabusa, III for infrared spectra. We wish to acknowledge the National Science Foundation (DMR-9310642 and DMR-9617477 to P.L.R. and CHE-9412387 to C.T.) for support of this research and the Kresge Foundation and donors to the Kresge Challenge program at the University of Akron for funds used to purchase the 600 MHz NMR instrument used in this work.

JA9831812